


Article

# Relation between Morphology and Porous Structure of SAPO-11 Molecular Sieves and Chemical and Phase Composition of Silicoaluminophosphate Gels

Marat R. Agliullin <sup>1,2,\*</sup>, Roman E. Yakovenko <sup>3</sup>, Yury G. Kolyagin <sup>4</sup> , Dmitry V. Serebrennikov <sup>1,\*</sup>, Farkhad S. Vildanov <sup>2</sup>, Tatyana R. Prosochkina <sup>2</sup> and Boris I. Kutepov <sup>1,2</sup>

<sup>1</sup> Institute of Petrochemistry and Catalysis, Ufa Federal Research Centre of the Russian Academy of Sciences (UFRC RAS), 450075 Ufa, Russia; kutepoff@inbox.ru

<sup>2</sup> Faculty of Chemical Engineering, Ufa State Petroleum Technological University, 450062 Ufa, Russia; stratpro@yandex.ru (F.S.V.); agidel@ufanet.ru (T.R.P.)

<sup>3</sup> Research Institute “Nanotechnologies and New Materials”, M.I. Platov South-Russian State Polytechnic University, 346428 Novocherkassk, Russia; yakovenko39@gmail.com

<sup>4</sup> Department of Chemistry, Moscow State University, 119991 Moscow, Russia; kolyagin@mail.ru

\* Correspondence: maratradikovich@mail.ru (M.R.A.); d25c25@yandex.ru (D.V.S.)

**Abstract:** The formation of silicoaluminophosphate gels using boehmite, Al isopropoxide, and di-n-propylamine as a template of silicoaluminophosphate gels as well as their subsequent crystallization into SAPO-11 molecular sieves was studied in detail using X-ray fluorescence spectroscopy (XRF), powder X-ray diffraction (XRD), Raman spectroscopy, scanning electron microscopy (SEM), transmission electron microscopy (TEM), and N<sub>2</sub> adsorption–desorption methods. The effect of the chemical and phase composition of silicoaluminophosphate gels on the physicochemical properties of SAPO-11 molecular sieves was shown. The secondary structural units that the AEL lattice is composed of were found to be formed at the initial stage of preparation involving aluminum isopropoxide. Several approaches to control their morphology and secondary porous structure are also proposed.

**Keywords:** silicoaluminophosphate gels; zeolites; SAPO-11; crystal morphology; micro-mesoporous materials



**Citation:** Agliullin, M.R.; Yakovenko, R.E.; Kolyagin, Y.G.; Serebrennikov, D.V.; Vildanov, F.S.; Prosochkina, T.R.; Kutepov, B.I. Relation between Morphology and Porous Structure of SAPO-11 Molecular Sieves and Chemical and Phase Composition of Silicoaluminophosphate Gels. *Gels* **2022**, *8*, 142. <https://doi.org/10.3390/gels8030142>

Academic Editors: Mazeyar Parvinezadeh Gashti and Jordi Puiggali

Received: 24 December 2021

Accepted: 16 February 2022

Published: 24 February 2022

**Publisher’s Note:** MDPI stays neutral with regard to jurisdictional claims in published maps and institutional affiliations.



**Copyright:** © 2022 by the authors. Licensee MDPI, Basel, Switzerland. This article is an open access article distributed under the terms and conditions of the Creative Commons Attribution (CC BY) license (<https://creativecommons.org/licenses/by/4.0/>).

## 1. Introduction

The current progress in oil refining and petrochemical industries is largely associated with the use of zeolites in the development of modern catalysts and adsorbents [1,2]. The widespread application of zeolites in the chemical industry is based on a successful combination of strong Brønsted acid sites and a developed microporous structure providing a molecular sieve effect [3]. As a rule, most of the zeolites employed in industrial processes are aluminosilicates in terms of chemical composition.

In 1984, Wilson et al. first reported on the synthesis of SAPO-n silicoaluminophosphate molecular sieves [4–6]. SAPO-n are characterized by a wide variety of structures differing in pore size (SAPO-18 3.8 × 3.8 Å, SAPO-5 7.3 × 7.3 Å, VPI-5 12.7 × 12.7 Å) and channel dimensions (1D SAPO-11, 2D SAPO-40, 3D SAPO-50) [7]. The Brønsted and Lewis acid sites in SAPO-n are formed as a result of the isomorphic insertion of silicon atoms into the aluminophosphate lattice during crystallization.

Currently, molecular sieves based on SAPO-n silicoaluminophosphates are already used in industry. In particular, UOP and the Dalian Institute of Chemical Physics (DICP) have developed and implemented industrial processes on the basis of SAPO-34 to obtain lower olefins from methanol [8]. Chevron has introduced a process for isodewaxing oils on the basis of SAPO-11 [9,10].

Among the wide variety of SAPO-n, SAPO-11 molecular sieves (AEL structure) are of particular interest due to the presence of a one-dimensional channel system with elliptical

pores of  $4.0 \times 6.5 \text{ \AA}$ , which are comparable to the molecular sizes of various practically important compounds and moderately strong acid sites. SAPO-11 molecular sieves are the most selective catalysts for hydroisomerization of  $C_{7+}$  n-paraffins [11–13], isomerization of n-butene to isobutylene [14] and cyclohexanone oxime to caprolactam [15,16] as well as the methylation of aromatic hydrocarbons [17,18].

Despite some success achieved in the synthesis and application of SAPO-11 molecular sieves in catalysis, the issues of formation and the relation between the results of subsequent crystallization of reaction gels and their physicochemical properties have been poorly studied thus far. Addressing these issues will make it possible to specify SAPO-11 crystallization and proceed to the development of these materials with the desired properties, which is one of the current challenges in the field of synthesis and research of molecular sieves.

Already in [19], phosphoric acid was found to react predominantly with an amine in the preparation of aluminophosphate reaction gels using boehmite as a source of Al. In this case, a gel of a complex composition is formed. However, the chemical and phase composition and their influence on the subsequent crystallization of  $AlPO_4$ -11 were not studied in this work.

It was shown in [20] that, upon stirring the gel at room temperature for up to 3 h, non-porous tridymite is formed in the process of further crystallization. Increasing the duration to 6 h results in the formation of SAPO-11 of high phase purity in a higher yield.

Earlier [16,21,22], we demonstrated that the reactivity of the Al source had a significant impact on the crystal morphology and secondary porous structure of the forming  $AlPO_4$ -11 molecular sieves.

The research results prove the importance of the gel formation stage during subsequent crystallization of the above materials. Therefore, we carried out a detailed study of the relation between the chemical and phase composition of silicoaluminophosphate gels prepared using various sources of aluminum and different contents of the template, and the morphology and porous structure of SAPO-11 molecular sieves formed during crystallization.

## 2. Results and Discussion

Tables 1 and 2 detail the chemical composition of the reaction gels and crystallization products based on them. The silicon content in the initial gels turned out to be higher than in the crystallization products. The fact that some of the silicon is not incorporated into the crystal lattice and remains in the mother liquor after crystallization accounts for the results obtained.

**Table 1.** Chemical and phase composition of silicoaluminophosphate gels.

Sample	Gel	pH Gel	Phase Composition
	$Al_2O_3 \cdot P_2O_5 \cdot SiO_2$		
SAPO-iAl-1.0	1.00·1.02·0.29	7.1	SAPO
SAPO-iAl-1.5	1.00·0.99·0.28	8.2	Layered.SAPO+SAPO
SAPO-PB-1.0	1.00·1.03·0.29	3.0	Ph.DPA+PB
SAPO-PB-1.0(60)	1.00·1.01·0.30	3.5	Ph.DPA+PB
SAPO-PB-1.0(90)	1.00·1.01·0.29	5.9	Ph.DPA+ $AlPO_4 \cdot 2H_2O$
SAPO-PB-1.0(120)	1.00·1.00·0.29	7.3	$AlPO_4 \cdot 2H_2O$
SAPO-PB-1.5	1.00·1.02·0.28	5.4	Ph.DPA+PB

Gel—Chemical composition of silicoaluminophosphate gels. SAPO—amorphous silicoaluminophosphate. Layered. SAPO—silicoaluminophosphate with a layered structure. Ph. DPA—di-n-propylamine phosphate. PB—boehmite.

**Table 2.** Chemical and phase composition of crystallization products.

Sample	Cryst.Prod	Phase Composition	DR, %
	$\text{Al}_2\text{O}_3 \cdot \text{P}_2\text{O}_5 \cdot \text{SiO}_2$		
SAPO-11-iAl-1.0	1.00-1.01-0.22	SAPO-11	87
SAPO-11-iAl-1.5	1.00-0.94-0.28	SAPO-11+SAPO-41	90
SAPO-11-PB-1.0	1.00-0.99-0.14	SAPO-11+Tr	-
SAPO-11-PB-1.0(60)	1.00-0.98-0.16	SAPO-11+Tr	-
SAPO-11-PB-1.0(90)	1.00-0.96-0.22	SAPO-11	95
SAPO-11-PB-1.0(120)	1.00-0.97-0.19	SAPO-11	97
SAPO-11-PB-1.5	1.00-0.98-0.17	SAPO-11+Tr	-

Cryst.Prod—crystallization products. Ph. DPA—di-n-propylamine phosphate. PB—boehmite. Tr—tridymite. DR—degree of crystallinity.

Figure 1 illustrates the X-ray diffraction patterns of dried gels; the phase composition is given in Table 1. In fact, the samples of gels prepared using boehmite, regardless of the content of the template, are a mixture of phases of di-n-propylamine phosphate and undissolved boehmite. The results indicate a weak interaction between sources of aluminum and phosphorus at the initial stage of the preparation of reaction gels. The gel samples prepared using Al isopropoxide, depending on the template content, can either be amorphous (SAPO-iAl-1.0 sample) or a mixture of phases of crystalline layered and amorphous silicoaluminophosphate (SAPO-iAl-1.5 sample).

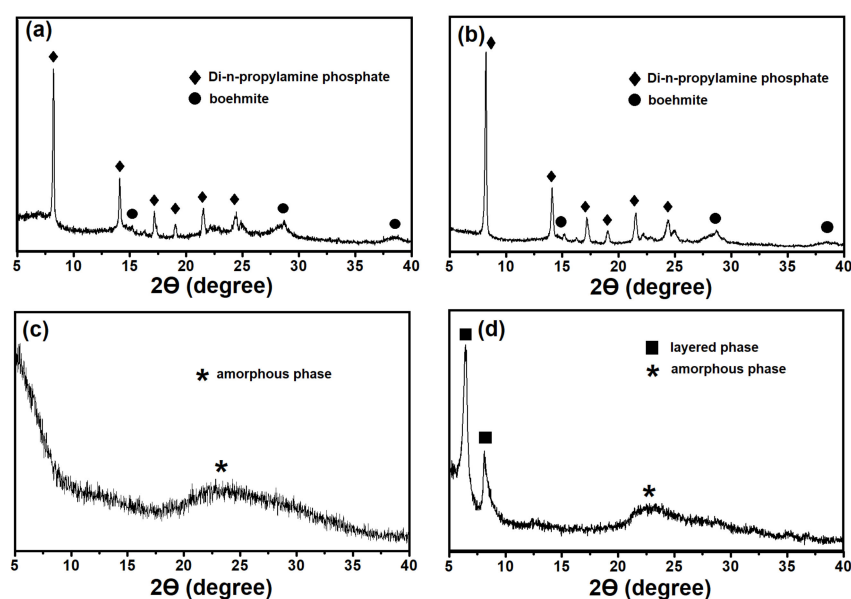


**Figure 1.** X-ray diffraction patterns of the silicoaluminophosphate gels: (a) Sample SAPO-PB-1.0; (b) Sample-SAPO-PB-1.5; (c) Sample-SAPO-iAl-1.0; (d) Sample-SAPO-iAl-1.5.

It should be noted that the pH value of the gels strongly depends on the reactivity of the Al source and the content of the template. Thus, when preparing gels using the more reactive Al isopropoxide, when aluminophosphate is formed already at the initial stages of their formation, the pH value exceeds  $\sim 7$ . When using a less reactive boehmite, it is  $\sim 5$ , even at a DPA/ $\text{Al}_2\text{O}_3$  ratio of 1.5.

Differences in the phase composition of gels affect the phase composition of the products of their crystallization (Figure 2). The SAPO-11 phase with an admixture of non-porous tridymite is formed from the samples of gels prepared on the basis of boehmite, regardless of the template content. During crystallization of the gels prepared using

aluminum isopropoxide, only molecular sieves are formed. Meanwhile, SAPO-11 of high phase purity is formed from the SAPO-iAl-1.0 gel, while SAPO-11 with SAPO-41 impurities is formed from the SAPO-iAl-1.5 gel.

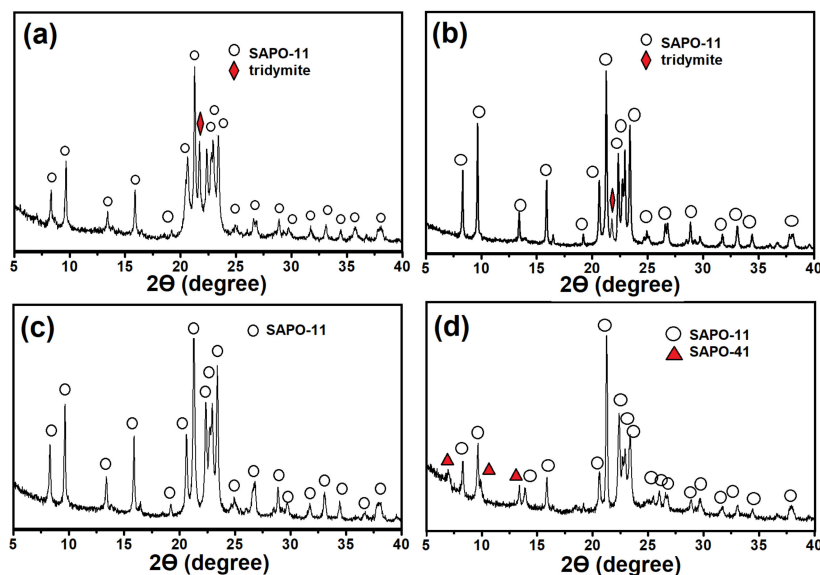


**Figure 2.** X-ray diffraction patterns of the products of crystallization of silicoaluminophosphate gels: (a) Sample SAPO-11-PB-1.0; (b) Sample-SAPO-11-PB-1.5; (c) Sample-SAPO-11-iAl-1.0; (d) Sample-SAPO-11-iAl-1.5.

Thus, crystallization of SAPO-11 of high phase purity is possible only from amorphous SAPO-11-iAl-1.0 gel under  $DPA/Al_2O_3$  ratio = 1.0. When it increases to 1.5, the conditions favorable for the formation of SAPO-41 are achieved. It is important to note that in the amorphous and layered phase, the sources of aluminum and phosphorus almost completely reacted with each other with the formation of bonds of the Al–O–P type, in contrast to gels prepared using boehmite.

As noted above, the gels prepared using aluminum isopropoxide are characterized by the presence of the Al–O–P type bonds. Raman spectroscopy is known to be very sensitive to ring structures forming the molecular sieve lattice. For  $AlPO_4-n$  and SAPO- $n$  molecular sieves, signals at 270 and 500  $cm^{-1}$  are associated with 10R and 4R rings [23,24]. The indicated bands were observed in the spectra of the SAPO-iAl-1.0 and iAl-1.5 samples (Figure 3). For SAPO-iAl-1.5, an additional band was observed at 270  $cm^{-1}$ , linked by 10R rings. Thus, future fragments of the SAPO-11 structure are formed at the initial stage of the preparation of the silicoaluminophosphate gel at room temperature.

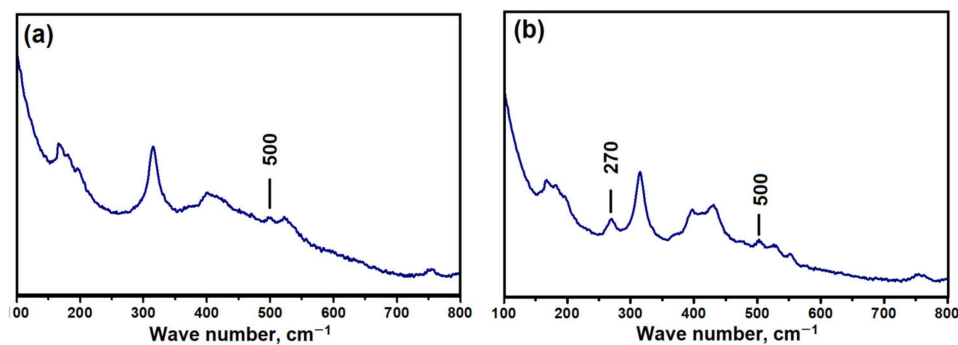
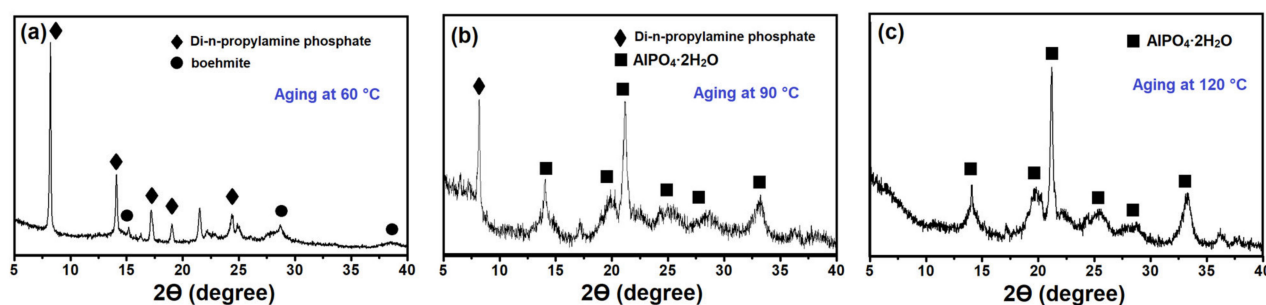


**Figure 3.** Raman spectra of silicoaluminophosphate gels: (a) Sample-SAPO-iAl-1.0; (b) Sample-SAPO-iAl-1.5.

In summary, the above results revealed that to prepare molecular sieves of high phase purity of the AEL structure, it is necessary that the main phases in the initial gels are aluminophosphates, which have already preformed the Al–O–P type bonds, contributing to the formation of crystals of the SAPO-11 molecular sieve.

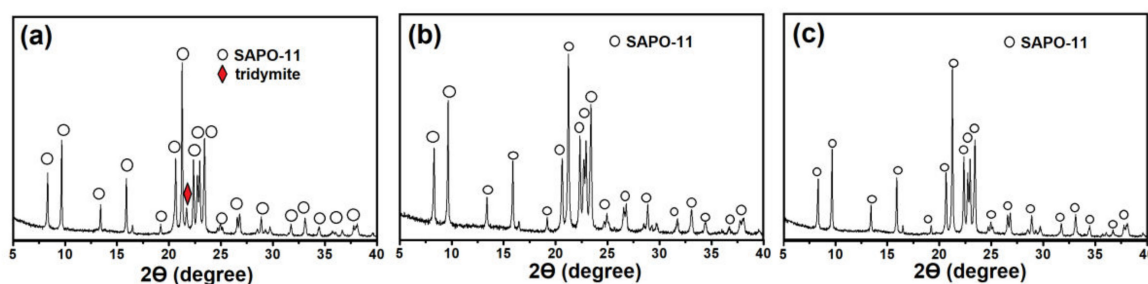
The solution to the problem of synthesizing SAPO-11 of high phase purity from initial gels prepared using such sources of Al as hydrated aluminum oxides (boehmite and pseudoboehmite) can be the introduction of an additional aging stage, which will preliminarily form a higher content of aluminophosphates.

Figure 4 shows the X-ray diffraction patterns of the gel samples aged at different temperatures. When increasing the aging temperature from 25 to 60 °C, practically no decrease in the intensity of signals characteristic of di-n-propylamine phosphate and undissolved boehmite was observed. The results obtained reveal a weak interaction of the indicated reagents. A further increase in the aging temperature from 90 to 120 °C brings about the appearance of an amorphous phase and hydroaluminophosphate  $\text{AlPO}_4 \cdot 2\text{H}_2\text{O}$  in the gels. Introduction of the aging stage at 90 and 120 °C therefore provides formation of predominantly aluminophosphate phases in the initial gels.



**Figure 4.** X-ray diffraction patterns of silicoaluminophosphate gels subjected to aging at different temperatures: (a) Sample SAPO-PB-1.0(60); (b) Sample-SAPO-PB-1.0(90); (c) Sample-SAPO-PB-1.0(120).

Figure 5 illustrates X-ray diffraction patterns of gel crystallization products subjected to aging. The gel crystallization products exposed to 90 and 120 °C were found to contain only signals characteristic of SAPO-11. The X-ray diffraction pattern of gel crystallization products aged at 60 °C exhibited additional signals typical for tridymite. Thus, the research results fully confirm our assumption about the need for the presence of aluminophosphate phases in the initial gels with already formed Al–O–P type bonds, providing selective crystallization of SAPO-11.



**Figure 5.** X-ray diffraction patterns of crystallization products of silicoaluminophosphate gels subjected to aging: (a) Sample SAPO-11-PB-1.0(60); (b) Sample-SAPO-11-PB-1.0(90); (c) Sample-SAPO-11-PB-1.0(120).

It is important to note that the results of crystallization significantly depend on the chemical and phase composition of the gels, which determine the pH value. Thus, SAPO-11 SAPO-PB-1.0(120) gel samples and SAPO-PB-1.5 SAPO-PB-1.0(90) gel samples were

characterized by pH values of  $\sim 7$  and  $\sim 5$ , respectively, while the results of their crystallization were significantly different from each other. As will be shown below, both the morphology of the crystals and the characteristics of their porous structure differed significantly.

Figure 6 shows the SEM images of dried silicoaluminophosphate gels. SAPO-PB-1.0 is a dense homogeneous material consisting of a mixture of di-n-propylamine phosphate and undissolved boehmite phases, as above-mentioned. The structure of the SAPO-PB-1.5 gel sample with a similar phase composition was composed of aggregates of nanosized particles. The gel samples aged at 90 and 120 °C were spherical aggregates ranging from 10 to 15  $\mu\text{m}$  in size. Higher magnification revealed that the structure of these materials was similar to a spongy structure, characterized by a developed system of pores ranging from 50 to 200 nm in size. An amorphous gel sample prepared using aluminum isopropoxide SAPO-iAl-1.0 resembled a xerogel in structure. According to the TEM data (Figure 7), the particles were formed of spherical particles of amorphous silicoaluminophosphate ranging from 10 to 20 nm in size. The structure of the SAPO-iAl-1.0 sample seems to be very close to the structure of silica gel and its formation proceeded through the sol–gel synthesis. The aluminophosphate SAPO-iAl-1.5 sample with a layered structure is represented by intergrowths of layers of various thicknesses. The TEM image shows that its structure was formed of thin plates resembling paper glued in several layers.

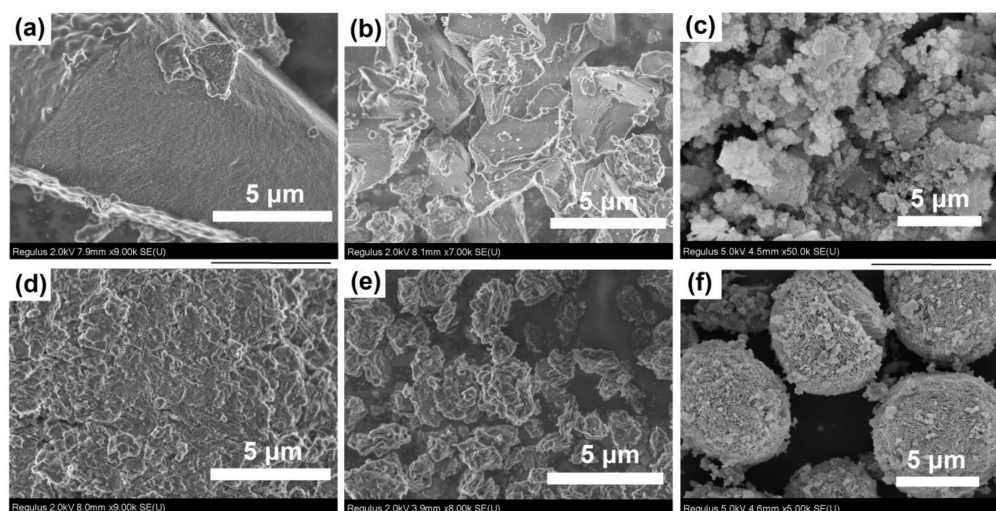


**Figure 6.** SEM image of silicoaluminophosphate gels: (a) Sample SAPO-PB-1.0; (b) Sample-SAPO-PB-1.5; (c) Sample-SAPO-iAl-1.0; (d) Sample-SAPO-iAl-1.5; (e) Sample-SAPO-PB-1.0(90); (f) Sample-SAPO-PB-1.0(120).

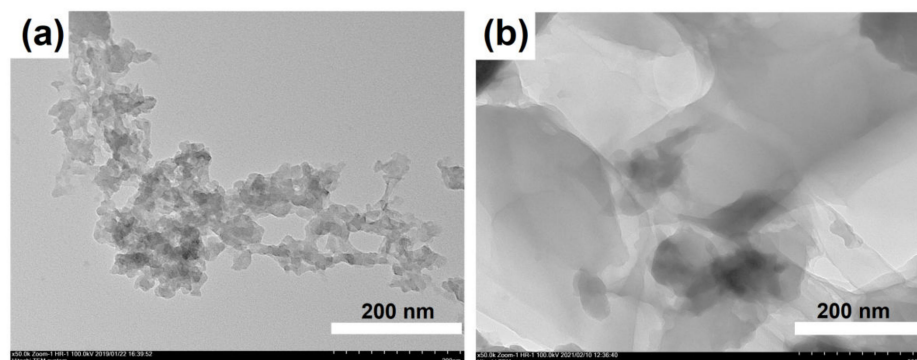


**Figure 7.** TEM image of silicoaluminophosphate gels: (a) Sample-SAPO-iAl-1.0; (b) Sample-SAPO-iAl-1.5.

Figure 8 shows images of gel crystallization products. Crystallization of SAPO-PB-1.0 gel prepared on the basis of boehmite resulted in the formation of SAPO-11 crystals, which are dense spherical aggregates of 6–8  $\mu\text{m}$  in size, consisting of densely packed nanosized crystals. An increase in the content of the template in the gel (SAPO-PB-1.5) brings about the appearance of a mixture of SAPO-11 crystals of various morphologies, namely, elongated needles, spherical intergrowths of nanocrystals, and hexagonal prisms. Furthermore, it should be noted that the introduction of the stage of aging SAPO-PB-1.0 gel at 90 or 120  $^{\circ}\text{C}$  fundamentally changes the morphology of SAPO-11. The SAPO-11-PB-1.0(90) sample was characterized by cubic crystals ranging from 100 to 500 nm in size, while the SAPO-11-PB-1.0(120) sample was characterized by crystals in the form of cones. The SAPO-11 sample prepared from amorphous gel (SAPO-iAl-1.0) was pseudospherical crystal aggregates of 6 to 8  $\mu\text{m}$  in size, consisting of smaller cubic crystals. Moreover, the crystals of the SAPO-11-iAl-1.5 sample obtained from a gel containing a layered phase were aggregates of thin plates forming an elongated cylinder of 6  $\mu\text{m}$  in size. It is noteworthy that the morphology of SAPO-11 crystals in the form of cones and elongated cylinders has not been previously reported.

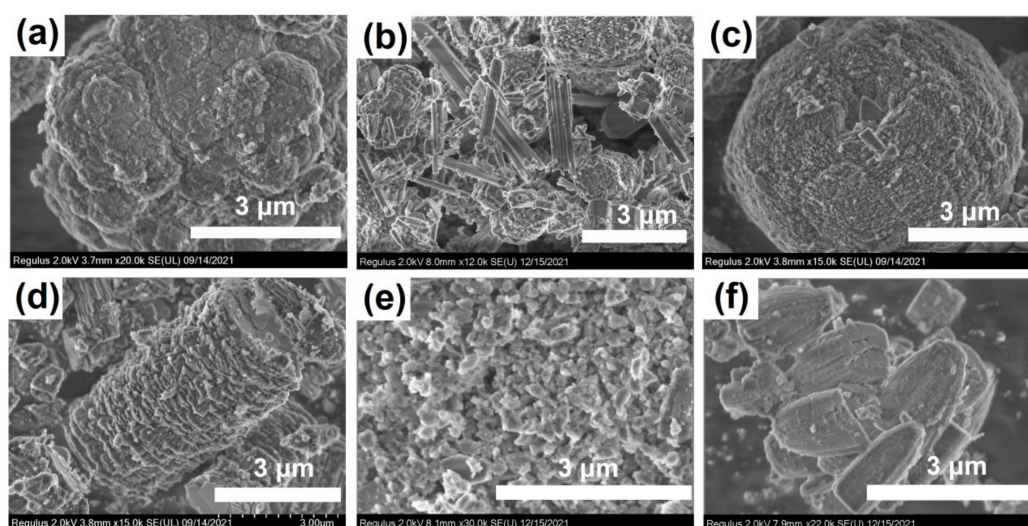


**Figure 8.** SEM image of crystallization products based on silicoaluminophosphate gels: (a) Sample SAPO-11-PB-1.0; (b) Sample-SAPO-11-PB-1.5; (c) Sample-SAPO-11-iAl-1.0; (d) Sample-SAPO-11-iAl-1.5; (e) Sample-SAPO-11-PB-1.0(90); (f) Sample-SAPO-11-PB-1.0(120).

Thus, the results obtained suggest that by regulating the chemical and phase composition of silicoaluminophosphate gels by using various sources of aluminum in their preparation and changing the content of the template in the reaction mixture as well as by introducing the aging stage, it is possible to control the morphology of primary crystals and secondary aggregates of SAPO-11 molecular sieves.

Figure 9 shows the nitrogen adsorption–desorption isotherms and pore size distribution; Table 3 lists the characteristics of the porous structure of the crystalline silicoaluminophosphate samples. For all SAPO-11 samples, type IV isotherms with a hysteresis loop close to the H4 type were observed. This type of isotherm is typical for micro-mesoporous materials. According to the BJH data, a wide distribution of mesopores of 2 to 25 nm in size was observed for all samples. The SAPO-11-PB-1.0 and SAPO-11-PB-1.5 samples were characterized by the smallest volume of micropores due to the presence of a non-porous tridymite phase in their composition. The introduction of the stage of aging the gel prepared using boehmite at 90  $^{\circ}\text{C}$  allows, upon further crystallization, one to synthesize the SAPO-11 sample with the highest specific surface area and mesopore volume. The results obtained are due to the fact that the secondary porous structure of this sample is formed of crystals ranging from 100 to 500 nm in size, which are only partially fused between.

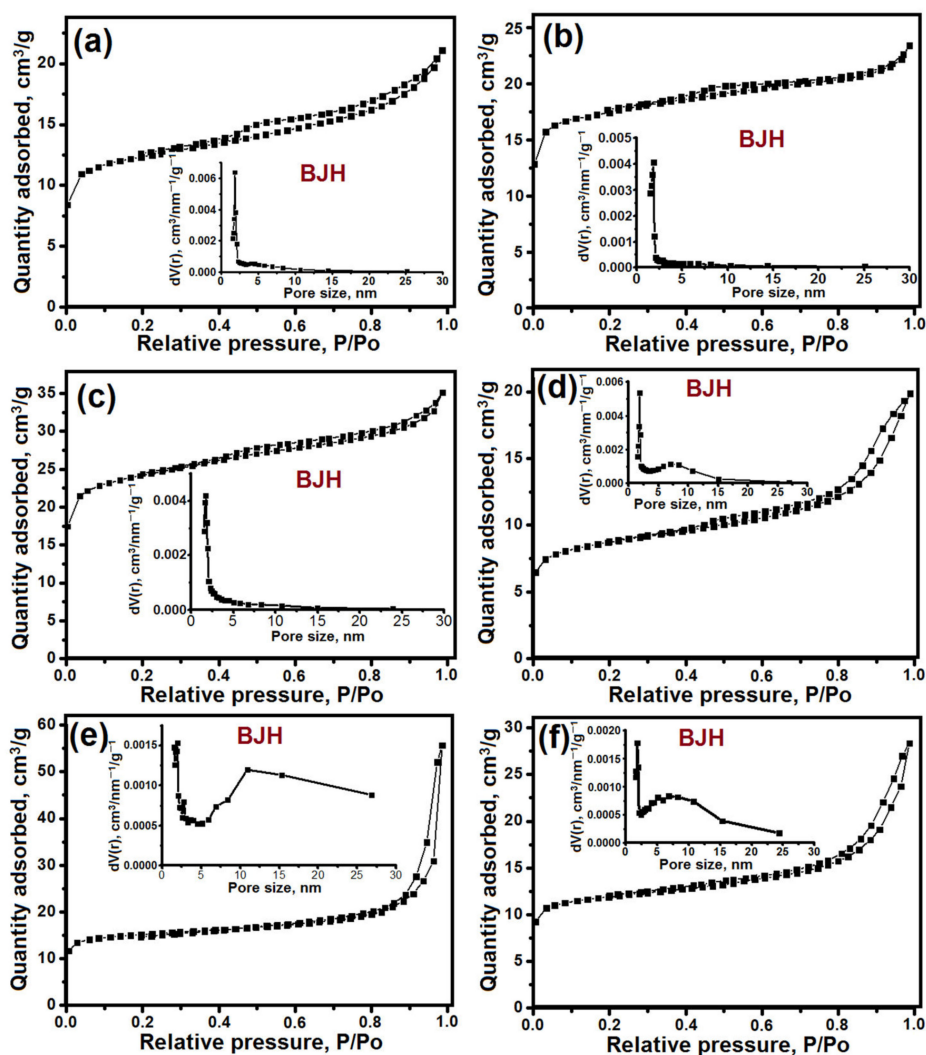


**Figure 9.** Nitrogen adsorption–desorption isotherms and pore size distribution (BJH) for the crystallization products based on silicoaluminophosphate gels: (a) Sample SAPO-11-PB-1.0; (b) Sample SAPO-11-PB-1.5; (c) Sample SAPO-11-iAl-1.0; (d) Sample SAPO-11-iAl-1.5; (e) Sample SAPO-11-PB-1.0(90); (f) Sample SAPO-11-PB-1.0(120).

**Table 3.** Characteristics of the porous structure of crystalline silicoaluminophosphates.

Sample	$S_{\text{BET}}$ , $\text{m}^2/\text{g}$	$S_{\text{EX}}$ , $\text{m}^2/\text{g}$	$V_{\text{micro}}$ , $\text{cm}^3/\text{g}$	$V_{\text{meso}}$ , $\text{cm}^3/\text{g}$
SAPO-11-PB-1.0	196	110	0.04	0.08
SAPO-11-PB-1.0	245	112	0.06	0.04
SAPO-11-PB-1.0(90)	250	120	0.07	0.27
SAPO-11-PB-1.0(120)	190	81	0.05	0.13
SAPO-11-iAl-1.0	250	127	0.07	0.06
SAPO-11-iAl-1.5	203	109	0.05	0.13

$S_{\text{BET}}$ —BET surface area.  $S_{\text{EX}}$ —external area.  $V_{\text{micro}}$ —micropore volume.  $V_{\text{meso}}$ —mesopore volume.

### 3. Conclusions

The influence of various sources of aluminum (boehmite, Al isopropoxide), the content of the template in the reaction mixture ( $\text{SDA}/\text{Al}_2\text{O}_3 = 1.0\text{--}1.5$ ), and as of the temperature ( $25\text{--}120\text{ }^\circ\text{C}$ ) aging stage on the chemical and phase composition as well as properties of the porous structure of silicoaluminophosphate gels and products of their subsequent



crystallization are detailed in the present work by applying the methods of XRD, Raman spectroscopy, SEM, TEM, and N<sub>2</sub> adsorption–desorption.

It has been established that an regulation of the chemical and phase composition of silicoaluminophosphate gels by changing the reactivity of the aluminum source, the content of the template in the reaction mixture as well as the temperature of the aging stage of silicoaluminophosphate gels makes it possible to address one of the current challenges in the field of the synthesis of molecular sieves with a hierarchical porous structure, namely, to develop approaches for the preparation of SAPO-11 molecular sieves of high phase purity with a hierarchical porous structure without using surfactants and various growth modifiers.

#### 4. Materials and Methods

##### 4.1. Preparation of Silicoaluminophosphate Gels

For the crystallization of SAPO-11 molecular sieves, we used silicoaluminophosphate gels with the following composition: 1.0Al<sub>2</sub>O<sub>3</sub>·1.0P<sub>2</sub>O<sub>5</sub>·0.3SiO<sub>2</sub> (1.0;1.5)DPA·40H<sub>2</sub>O. To prepare the gels, Al isopropoxide (iAl, 98%, Acros Organics, Noisy-le-Grand, France) or boehmite (PB, AlO(OH), Sasol SB, Hamburg, Germany), SiO<sub>2</sub> sol, orthophosphoric acid (H<sub>3</sub>PO<sub>4</sub>, 85%, Reachim, Moscow, Russia), and di-n-propylamine (DPA, 99%, Acros Organics, Schwerte, Germany) were used as sources of Al, P, Si, and a template, respectively. Silicoaluminophosphate gels were prepared as follows: 10.0 g of orthophosphoric acid was added to 27.0 g of distilled water and 17.3 g of Al isopropoxide or 5.6 g of boehmite was added under vigorous stirring to form alumophosphate, then 4.4 or 6.6 g of di-n-propylamine was added to the gel. After DPA was added, the calculated amount of the SiO<sub>2</sub> source was slowly introduced into the resulting gel, and then the reaction mixture was intensively stirred for 1 h.

Table 4 lists the designations of gel samples prepared using different sources of Al and different contents of the template. The aging temperature of the reaction gels is given in parentheses.

**Table 4.** Conventional designation of silicoaluminophosphate gels of various chemical composition and crystallization products.

Sample	Source Al	Gel Composition
SAPO-iAl-1.0	iAl	1.0Al <sub>2</sub> O <sub>3</sub> ·1.0P <sub>2</sub> O <sub>5</sub> ·0.3SiO <sub>2</sub> ·1.0DPA·40H <sub>2</sub> O
SAPO-iAl-1.5	iAl	1.0Al <sub>2</sub> O <sub>3</sub> ·1.0P <sub>2</sub> O <sub>5</sub> ·0.3SiO <sub>2</sub> ·1.5DPA·40H <sub>2</sub> O
SAPO-PB-1.0	PB	1.0Al <sub>2</sub> O <sub>3</sub> ·1.0P <sub>2</sub> O <sub>5</sub> ·0.3SiO <sub>2</sub> ·1.0DPA·40H <sub>2</sub> O
SAPO-PB-1.0(90)	PB	1.0Al <sub>2</sub> O <sub>3</sub> ·1.0P <sub>2</sub> O <sub>5</sub> ·0.3SiO <sub>2</sub> ·1.0DPA·40H <sub>2</sub> O
SAPO-PB-1.0(120)	PB	1.0Al <sub>2</sub> O <sub>3</sub> ·1.0P <sub>2</sub> O <sub>5</sub> ·0.3SiO <sub>2</sub> ·1.0DPA·40H <sub>2</sub> O
SAPO-PB-1.5	PB	1.0Al <sub>2</sub> O <sub>3</sub> ·1.0P <sub>2</sub> O <sub>5</sub> ·0.3SiO <sub>2</sub> ·1.5DPA·40H <sub>2</sub> O
SAPO-11-iAl-1.0	iAl	1.0Al <sub>2</sub> O <sub>3</sub> ·1.0P <sub>2</sub> O <sub>5</sub> ·0.3SiO <sub>2</sub> ·1.0DPA·40H <sub>2</sub> O
SAPO-11-iAl-1.5	iAl	1.0Al <sub>2</sub> O <sub>3</sub> ·1.0P <sub>2</sub> O <sub>5</sub> ·0.3SiO <sub>2</sub> ·1.5DPA·40H <sub>2</sub> O
SAPO-11-PB-1.0	PB	1.0Al <sub>2</sub> O <sub>3</sub> ·1.0P <sub>2</sub> O <sub>5</sub> ·0.3SiO <sub>2</sub> ·1.0DPA·40H <sub>2</sub> O
SAPO-11-PB-1.5	PB	1.0Al <sub>2</sub> O <sub>3</sub> ·1.0P <sub>2</sub> O <sub>5</sub> ·0.3SiO <sub>2</sub> ·1.5DPA·40H <sub>2</sub> O

##### 4.2. Aging of Silicoaluminophosphate Gels

The samples of SAPO-PB-1.0 silicoaluminophosphate gel were kept in a thermostat at 60, 90, or 120 °C for 24 h. After aging, the gel samples were assigned an additional index (60), (90), and (120), respectively (Table 3).

##### 4.3. Crystallization of SAPO-11 Molecular Sieves

SAPO-11 molecular sieves were crystallized from the corresponding silicoaluminophosphate gels at 200 °C for 24 h. Preliminary experiments have shown that crystallization for

more than 24 h results in the formation of cristobalite. Table 3 lists the designations of the SAPO-11 samples obtained from silicoaluminophosphate gels of various compositions.

#### 4.4. Methods of Material Analysis

The chemical composition of the obtained silicoaluminophosphate gels and crystallization products was characterized by X-ray fluorescence spectroscopy recorded on a Shimadzu EDX 7000P spectrometer (Duisburg, Germany) by the fundamental parameter method.

Powder X-ray diffraction patterns of silicoaluminophosphate gels and the uncalcined SAPO-11 samples were recorded on a Bruker D8 Advance diffractometer (Karlsruhe, Germany) in  $\text{CuK}\alpha$  radiation. The patterns were collected over a  $2\theta$  range from 5 to  $40^\circ$  with a scanning speed of  $1^\circ$  min. The phase analysis of the obtained X-ray diffraction patterns was performed by the DIFFRAC.EVA program using the PDF2 database. The crystallinity degree was assessed by the content of an amorphous halo in the range from 20 to  $30^\circ(2\theta)$ .

Raman spectra of the silicoaluminophosphate gels were obtained on a FT-Raman Thermo Scientific Nicolet NXR 9650 Fourier spectrometer (Waltham, MA, USA) in the range of  $70\text{--}3800\text{ cm}^{-1}$  with a resolution of  $2\text{ cm}^{-1}$ . An Nd:YVO<sub>4</sub> laser with a wavelength of 1064 nm and a power up to 1.5 W was used as an excitation source.

The size and morphological features of silicoaluminophosphate gels and SAPO-11 were detailed by field emission scanning electron microscopy (FE-SEM) with a Hitachi Regulus SU8220 scanning electron microscope (Tokyo, Japan). The images were taken in the mode of registration of secondary electrons at 2 kV accelerating voltage. The microstructure of the samples was also examined by transmission electron microscopy (TEM) on a Hitachi HT 7700 electron microscope (Tokyo, Japan). The images were recorded in the light field mode at an accelerating voltage of 100 kV.

The BET surface area, the volume of micro- and mesopores were measured by the method of low-temperature nitrogen adsorption–desorption with a Nova 1200e sorptometer (Quantachrome Instruments, Boynton Beach, FL, USA). The specific surface area was calculated by the multipoint BET method. The micropore volumes in the presence of mesopores were derived from a *t*-Plot approach. The pore size distribution was calculated by the BJH (Barrett–Joyner–Halendy) model from the desorption branch. Prior to the analysis, fresh samples were calcined at  $600^\circ\text{C}$  for 6 h.

**Author Contributions:** Conceptualization, M.R.A.; Methodology, M.R.A.; Validation, M.R.A.; Investigation, M.R.A., Y.G.K., R.E.Y. and D.V.S.; Writing—Original Draft Preparation, M.R.A.; Writing—Review & Editing, M.R.A., T.R.P. and D.V.S.; Supervision, B.I.K. Funding Acquisition, F.S.V. All authors have read and agreed to the published version of the manuscript.

**Funding:** This research was funded by the Russian Science Foundation No. 21-73-00013.

**Institutional Review Board Statement:** Not applicable.

**Informed Consent Statement:** Not applicable.

**Data Availability Statement:** Not applicable.

**Conflicts of Interest:** The authors declare no conflict of interest.

## References

1. Martinez, C.; Corma, A. Inorganic molecular sieves: Preparation, modification and industrial application in catalytic processes. *Coord. Chem. Rev.* **2011**, *255*, 1558–1580. [\[CrossRef\]](#)
2. Vermeiren, W.; Gilson, J.-P. Impact of zeolites on the petroleum and petrochemical industry. *Top. Catal.* **2009**, *52*, 1131–1161. [\[CrossRef\]](#)
3. Cejka, J.; Corma, A.; Zones, S. *Zeolites and Catalysis: Synthesis Reactions and Applications*; Wiley—VCH Verlag, GmbH & Co. KGaA: Weinheim, Germany, 2010; pp. 1–881. [\[CrossRef\]](#)
4. Lok, B.M.; Messina, C.A.; Patton, R.L.; Gajek, R.T.; Cannan, T.R.; Flanigen, E.M. Crystalline Silicoaluminophosphates. U.S. Patent 4,440,871, 3 April 1984.

5. Flanigen, E.M.; Lok, B.M.; Patton, R.L.; Wilson, S.T. Aluminophosphate molecular sieves and the periodic table. *Stud. Surf. Sci. Catal.* **1986**, *28*, 103–112. [[CrossRef](#)]
6. Wilso, S.T.; Lok, B.M.; Messina, C.A.; Cannan, T.R.; Flanigen, E.M. Aluminophosphate molecular sieves: A new class of microporous crystalline inorganic solids. *J. Am. Chem. Soc.* **1982**, *104*, 1146–1147. [[CrossRef](#)]
7. Baerlocher, C.; Meier, W.M.; Olson, D.H. *Atlas of Zeolite Framework Types*, 6th ed.; Elsevier: Amsterdam, The Netherlands, 2007; pp. 1–404.
8. Yang, M.; Fan, D.; Wei, Y.; Tian, P.; Liu, Z. Recent Progress in Methanol-to-Olefins (MTO) Catalysts. *Adv. Mater.* **2019**, *31*, 1902181. [[CrossRef](#)] [[PubMed](#)]
9. Miller, S.J. New molecular sieve process for lube dewaxing by wax isomerization. *Microporous Mater.* **1994**, *2*, 439–449. [[CrossRef](#)]
10. Miller, S.J. Studies on Wax Isomerization for Lubes and Fuels. *Stud. Surf. Sci. Catal.* **1994**, *84*, 2319–2326. [[CrossRef](#)]
11. Yadav, R.; Sakthivel, A. Silicoaluminophosphate molecular sieves as potential catalysts for hydroisomerization of alkanes and alkenes. *Appl. Catal. A Gen.* **2014**, *481*, 143–160. [[CrossRef](#)]
12. Deldari, H. Suitable catalysts for hydroisomerization of long-chain normal paraffins. *Appl. Catal. A Gen.* **2005**, *293*, 1–10. [[CrossRef](#)]
13. Wang, W.; Liu, C.-J.; Wu, W. Bifunctional catalysts for the hydroisomerization of *n*-alkanes: The effects of metal–acid balance and textural structure. *Catal. Sci. Technol.* **2019**, *9*, 4162–4187. [[CrossRef](#)]
14. Meriaudeau, P.; Vu Tuan, A.; Le Hung, N.; Szabo, G. Skeletal isomerisation of 1-butene on 10-member ring zeolites or on 10-member ring silico-alumino-phosphate microporous materials. *Catal. Lett.* **1997**, *47*, 71–72. [[CrossRef](#)]
15. Singh, P.S.; Bandyopadhyay, R.; Hegde, S.G.; Rao, B.S. Vapour phase beckmann rearrangement of cyclohexanone oxime over SAPO-11 molecular sieve. *Appl. Catal. A Gen.* **1996**, *136*, 249–263. [[CrossRef](#)]
16. Agliullin, M.R.; Faizullin, A.V.; Khazipova, A.N.; Kutepov, B.I. Synthesis of Fine-Crystalline SAPO-11 Zeolites and Analysis of Their Physicochemical and Catalytic Properties. *Kinet. Catal.* **2020**, *61*, 654–662. [[CrossRef](#)]
17. Zhu, Z.; Chen, Q.; Xie, Z.; Yang, W.; Li, C. The roles of acidity and structure of zeolite for catalyzing toluene alkylation with methanol to xylene. *Micropor. Mesopor. Mater.* **2006**, *88*, 16–21. [[CrossRef](#)]
18. Wang, X.; Guo, F.; Wei, X.; Liu, Z.; Zhang, W.; Guo, S.; Zhao, L. The catalytic performance of methylation of naphthalene with methanol over SAPO-11 zeolites synthesized with different Si content. *Korean J. Chem. Eng.* **2016**, *33*, 2034–2041. [[CrossRef](#)]
19. Tapp, N.J.; Milestone, N.B.; Bibby, D.M. Synthesis of AlPO<sub>4</sub>-11. *Zeolites* **1988**, *8*, 183–188. [[CrossRef](#)]
20. Lopez, C.M.; Escobar, V.; Arcos, M.E.; De Nobrega, L.; Yáñez, F.; Garcia, V.L. Synthesis, characterization and catalytic behaviour of SAPO-11 obtained at low crystallization times and with low organic agent content. *Catal. Today* **2008**, *133–135*, 120–128. [[CrossRef](#)]
21. Agliullin, M.R.; Khairullina, Z.R.; Faizullin, A.V.; Kutepov, B.I. Crystallization of AlPO<sub>4</sub>-11 Aluminophosphate from Various Aluminum Sources. *Pet. Chem.* **2019**, *59*, 349–353. [[CrossRef](#)]
22. Agliullin, M.R.; Lazarev, V.V.; Kutepov, B.I. Influence of the formation conditions of aluminophosphate gels on the morphology and pore structure of molecular sieve AlPO<sub>4</sub>-11. *Russ. Chem. Bull.* **2021**, *70*, 47–55. [[CrossRef](#)]
23. Yu, Y.; Xiong, G.; Li, C.; Xiao, F.-S. Characterization of aluminosilicate zeolites by UV Raman spectroscopy. *Microporous Mesoporous Mater.* **2001**, *46*, 23–34. [[CrossRef](#)]
24. Holmes, A.J.; Kirkby, S.J.; Ozin, G.A.; Young, D. Raman spectra of the unidimensional aluminophosphate molecular sieves AlPO<sub>4</sub>-11, AlPO<sub>4</sub>-5, AlPO<sub>4</sub>-8, and VPI-5. *J. Phys. Chem.* **1994**, *98*, 4677–4682. [[CrossRef](#)]